Journal of Marine Science and Engineering

MDPI

Article

Experimental Study on the Stability and Wave Force of a Breakwater transition under Multiangle Oblique Waves

Guang-sheng WANG[1], Long-zai GE[2]*, Tong YU[1], Ya-jing ZHANG[2]* and Song-gui CHEN[2]

1. China Harbor Engineer company LTD, Beijing100027, China;gswang@chec.bj.cn (G.S.);tyu@chec.bj.cn (Y.T.)
2. Tianjin Research Institute for Water Transport Engineering, National Engineering Research Center of Port Hydraulic Construction Technology, Tianjin 300456, China; chensg@tiwte.ac.cn (S.G.)

* Correspondence: gelz@tiwte.ac.cn (L.G.); zhyj@tiwte.ac.cn (Y.J.).

Abstract: Based on the failure and instability of different structural transition of offshore breakwater, provides a basis for understanding the instability mechanism and further providing engineering repair. Based on the breakwater project in the regulation of the bay of Shandong Province, physical model tests with a scale of 1:36 were carried out. This study revealed the wave characteristics, force performance, and instability mechanism in the transition. In the test, the relationships between 5 °, 15 °, 35 °, and 75 ° oblique waves, the wave force, and the stable weight of the Accropode were simulated, revealing that the generation of a shock wave current is related to the wave direction angle, resulting in the local wave height increasing by 2.05 times. The instability of the 8T and 2T Accropode designed for the breakwater was obtained, and they were stable after the optimization test. The wave force of the caisson of the transition was concentrated in the anti-arc section of the superstructure, and the maximum horizontal force, buoyancy force, and impact pressure were 935.6 kN, 419.1 kN, and 65.9kPa, respectively. The instability mechanism was determined as the poor connection between the accropode and the caisson, and the wave energy concentration. Compared with the calculation results of the standard formula, the correction coefficients of the overtopping volume, wave crest elevation, wave force, and Accropode weight at the transition of breakwater were 1.95, 1.97, 1.60, and 4.0, respectively. The test results have solved the practical problems of the project and can also provide reference for similar projects.

Keywords: oblique wave; transition area of different structures; stability; wave force; test methods

Citation: To be added by editorial staff during production.

Academic Editor: Firstname Lastname

Received: date
Accepted: date
Published: date

Publisher's Note: MDPI stays neutral with regard to jurisdictional claims in published maps and institutional affiliations.

Copyright: © 2022 by the authors. Submitted for possible open access publication under the terms and conditions of the Creative Commons Attribution (CC BY) license (https://creativecommons.org/licenses/by/4.0/).

1. Introduction

Waves contain huge amounts of energy. In order to block the direct effect of large waves in the open sea to ensure the utility of the water area in a port and the safety of the wharf and other infrastructure, it is usually necessary to build a breakwater. In recent years, with the development of port construction, the port site has gradually expanded from a natural bay with good natural conditions to the open sea, and breakwater construction has also had to face a harsh hydrodynamic environment.

Influenced by factors such as an increase in the water depth, the deterioration of wave conditions in offshore construction, and restrictions on the exploitation of backfill stones, designs propose the adoption of two different structural combinations of vertical caissons and breakwater at appropriate water depths [1-3]. However, in recent years, as the intensity of extreme sea conditions increases, at the transition of two structures, the failure accidents of breakwater instability occurred [4,5]. Figure 1(a) shows a breakwater transition in Guangdong Province of China that was damaged in a typhoon, causing huge economic losses to the enterprise [6]. As seen from the damaged site of the project in Figure 1, the instability mechanism of the failure of the breakwater transition was very different from that of other regions, and it was affected by more complex hydro-

dynamic forces and multiple factors of interaction superposition between the different structures.For Figure 1(a) shows the caisson sliding at the breakwater transition and the Accropode rolling down to the upper part of the caisson, resulting in the mixing of different structures; Figure1(b) shows the instability of the armour block,the main differences between the two types of breakwater instability are as follows: ① the hydrodynamic characteristics are different, the former has wave energy concentration and backwater; ② The connection of the armour block is different, the former is of two different structures, and the connection is poor, the latter is normal..



(**a**)



(**b**)

Figure1. Site damage and instability of breakwater: (**a**) damage of transition zone of different structures of breakwater; (**b**)damage of breakwater head with the same structure..

In order to understand the mechanism of breakwater failure and instability and to provide a basis for engineering repair, it is necessary to first verify the wave characteristics at the breakwater transition, establish the relationship between the characteristics of the wave and force and the stability weight of armor, compare it with the design value calculated by the standard formula to obtain the deviation between them, and then provide the corresponding correction coefficient.

Reference previous research results and focusing on the research on multiangle wave action at the transition, there are few relevant achievements at home and abroad at present, but there are many research results on the stability of the same structure armor block or wave force on the vertical caisson.

For the research on the stability of the breakwater armor under wave action, ZHANG et al. [7] pointed out that when oblique waves impact the stability of the seawall, the positions prone to instability due to the wave breaking are shown at the wave

side at the back of the breakwater head and the steep change in the topography at the bottom of the breakwater. CHANG et al. [8] used the action of normally-incident wave in their study of the stability of hollow square blocks at four corners and found the limitation of the formula for calculating the stable weight in the standard, proposing the model test results to provide a necessary supplement for the design basis.

JIANG et al. [9] used physical tests to point out that an oblique wave at a certain angle is more dangerous to the Accropode than a normal wave, and they proposed that the influence of the poor occlusion function of the armor should be considered for the lateral action. MORIMOTO [10] proposed that the resonance phenomenon caused by waves on breakwater is an important factor determining its stability conditions by means of experiments and designed experiments to explore the mechanism of wave action. WU et al. [11] determined the calculation method of the stability weight of a breakwater's bottom protection Accropode under the action of different oblique waves through theoretical analysis and test comparisons. Foreign scholars have conducted stability studies on the transition between a slope-type breakwater armor and a wave energy conversion device embedded in the breakwater using different submerged and oblique wave combinations; they obtained the instability mechanism of the armor between the two and analyzed the optimal location of the device on the breakwater body section [12-14].

~~According to the statistics of~~ calculation formulas derived by researchers in various countries regarding the armor stability weight under oblique wave action~~, there are mainly two categories~~. The methods adopted are based on the industry-recognized Equation (1)[15] for the armor stability weight under normal wave action, and the influence factors in Equation (1) are modified according to the characteristics of the oblique wave ~~action; that is, the first category modifies the wave height. The calculation formula obtained is shown~~ in Equation (2). The other way is to modify the stability coefficient, and the calculation formula is shown in Equation (3).

$$W/(\gamma_b H_s^3) = K_D f\left((\gamma_b - \gamma)/\gamma\right) f(m) \quad (1)$$

$$H_s = (H_s)_\theta (\sin\beta)^x \quad (2)$$

$$K_{D,\theta} = K_s K_D (\cos\theta)^{-\varepsilon} \quad (3)$$

where W is the stable weight of the armor; $K_{D,\theta}$ is the stability coefficient of the oblique action; γ_b and γ are the weight of the block and water, respectively; H_s is the design wave height; K_D is the stability coefficient of the armor; θ is the angle between the slope and horizontal; β is angle between wave incidence direction and breakwater axis; m is the slope gradient; K_s is the influence coefficient of the wave direction distribution; and ε is a parameter representing the influence of the wave incidence direction on the stability of the armor, which is generally between 1.0 and 1.1.

For the research results on wave forces acting on vertical caissons,ALLSOP [16] found through experimental research that the wave breaking impact force of oblique wave acting on the unit length of breakwater is smaller than that of normal wave, and the formula of wave breaking impact force reduction coefficient is given as follows:

$$\gamma_h = 1 - X(L_C - L_P) \quad (4)$$

Where, γ_h is the reduction coefficient, and X is the coefficient, When the incidence angles are 0°, 15° and 30° respectively, the corresponding coefficients are 1.35, 1.69 and 1.96. L_C is the unit dike length, and L_P is the wavelength of the spectral peak period.

BATTJES [17] used the linear theory to give the calculation formula of the reduction coefficient of the horizontal wave force acting on the unit breakwater along the longitudinal direction of the unit breakwater, but MADRIGAL pointed out that because the BATTJES theory ignored the nonlinear effect between the wave surface and the wave force, and underestimated the longitudinal reduction of the wave force, the conservative reduction coefficient was given, and the reduction coefficient formula was obtained as follows:

The longitudinal reduction coefficient of horizontal force is:

$$\gamma_h = 1 - 1.67(L_C sin(\beta)/L_P) \quad (5)$$

The longitudinal reduction coefficient of buoyancy force is:

$$\gamma_u = 1 - 0.99(L_C sin(\beta)/L_P) \quad (6)$$

In the empirical formula of GODA [18,19], the influence of one-way wave oblique action is considered by introducing relevant coefficients. The calculated wave force per unit breakwater length decreases monotonously with the increase of wave direction angle, but the influence of unit breakwater length on total wave force is not considered.

~~CHEN~~ [20] and CHEN et al. [21] conducted tests on the forces acting on vertical caissons using waves of different angles, pointing out that the oblique irregular wave forces acting on a unit length of the breakwater decreased with the increase in the wave direction angle. FRANCO [22] proposed that when the incident angle is less than 40°, compared with a normal wave force, the structural force can be multiplied by the reduction factor related to the wave angle. HONG [23] obtained the wave incidence angle ($\theta = 40°$) in an experimental study on the effect of oblique and multidirectional waves on open bed caisson breakwaters in a deep-water nonbroken sea area, and the wave force reached the maximum. MADRIGAL [24] established a mathematical model for the interaction between oblique incident nonlinear irregular waves and a vertical wall between the surface gravity wave and the vertical wall and obtained the relationship between the wave angle and the force. LI et al. [25], through a model test, obtained that the wave force on the structure decreased with the increase in the wave incidence angle, and they provided a formula for the reduction coefficient of the wave force on a unit length of breakwater. YU et al. [26] discussed the influence of the wave angle of the wave forces on vertical breakwaters based on an experimental study of a three-dimensional wave physical model, and they proposed a variation law between the wave angle and the structural forces under the condition of whether the waves were broken. They proposed a calculation formula between the wave angle and vertical structures. Through experiments and theoretical analysis, it was obtained that when the wave incidence angle is less than or equal to 45°, the wave force decreases with the increase in the incidence angle, and a formula that is conducive to the angle's calculation is provided [27,28]. WANG et al. [29] used the numerical simulation method to study the wave force analysis of the small-angle change in the wave face of a vertical breakwater, and they obtained the relationship between the angle and wave force, especially the influence of oblique waves. Some scholars have demonstrated the relationship between overtopping and the wave force of vertical caissons when extreme sea waves are vertically incident through physical model test results, numerical simulation,such overtopping waves and their accompanying wave forces can induce various mechanisms of structure failure that result in structural instability [30]. Extensive experimental studies have been conducted to estimate the forces and pressures that are induced by a tsunami bore and exerted on structures [31]. At present, the formulas are used most often for caisson design [32].

Similarly, the empirical formula for calculating the wave force and angle of a vertical caisson under oblique wave action by previous researchers is summarized, and the whole formula derivation process is as follows: establish the relationship with the angle (φ) according to Equation (7), obtain the reduction coefficient (k_p) of the force under an oblique wave, and then obtain the relationship between the wave force on a vertical caisson under an oblique wave and the wave height (H) and angle (β). See Equation (8) for the specific calculation formula.

$$k_\mathrm{p} = \frac{1+\sin(\beta-22.5°)}{2} \quad (7)$$

$$P = Bk_\mathrm{p}\frac{(H+h_\mathrm{s}+d_1)(p_\mathrm{b}+\gamma d_1)-\gamma d_1^2}{2} \quad (8)$$

where P is the total horizontal force; h_s is the height of the wave crest; d is the water depth; p_d is the bottom pressure; p_b is the bottom wave pressure of the caisson; d_1 is the water depth on the foundation bed; B is the bottom width of the caisson; and k_p is the reduction factor;H is incident wave height.

There are few studies on transition of breakwaters, but there are some results on the joints of other projects. For example, GE et al. [33] studied the stability of an armor block at the transition between an artificial island and an immersed tunnel under wave current coupling, and they obtained the relationship between the stability and the incident wave height under different wave current coupling angles. ~~ZHAGN~~ et al. [34] demonstrated the stability of an armor block using the transition between the breakwater and the near shore. GE et al. [35] provide the wave characteristics and structural stability of a breakwater connection section with the same breakwater structure. KUA et al. [36] provide the research results of a wave force and wave direction angle at a bridge bottom under different wave actions at the bridge and shore structure.

To sum up, the currently achievements rarely involve paying attention to the wave characteristics, the stability of armor and the wave forces of caissons at the breakwater transition at the same time. In addition, it is difficult to refer to the relevant provisions in the specification for design values. In view of this, a physical model test with a scale of 1:36 was carried out against the background of Shandong Rizhao Bay breakwater regulation project.

2. Model Test Design

2.1. Project background

Based on the Shandong Rizhao Bay breakwater project [37], in order to achieve coordination between the port and the city, it was proposed to restore the 1882 m(Note: prototype size, the same below.) shoreline of the port coal yard as the ecological coast of the artificial beach. At the same time, in order to resist the erosion of the artificial beach by strong waves from the open sea, an 885.4 m sand-retaining breakwater will be built. The project's layout is shown in Figure 2.

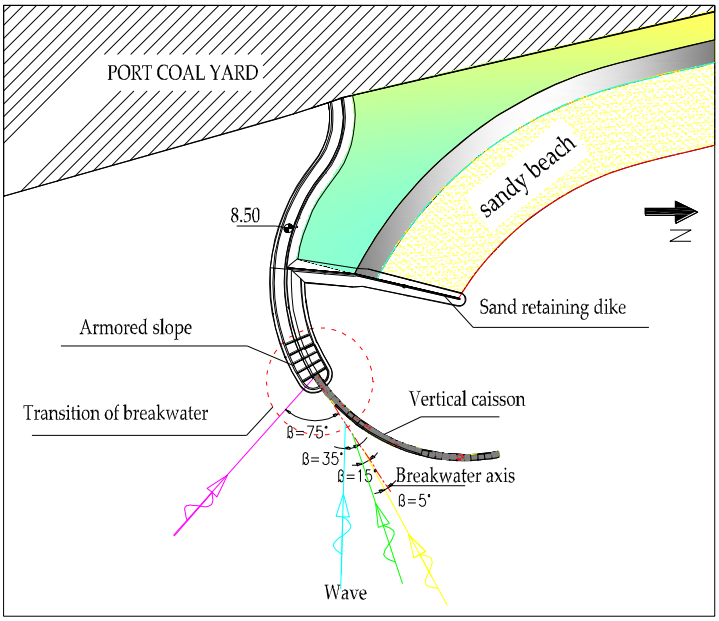


Figure 2. Layout plan of the transition of breakwater project.

Figure3 shows the structural section at the transition of breakwater. The dimensions of caisson are 18.66m (long) × 16.86 m(width) × 19.5 m (height); the top elevation is +8.5 m; The underwater terrain elevation of the breakwater transition area is between - 15.0m and -19.0m.8T Accropode is being used ~~for the slope structure armor block~~; and 2T Accropode ~~is~~ being used for the port side.

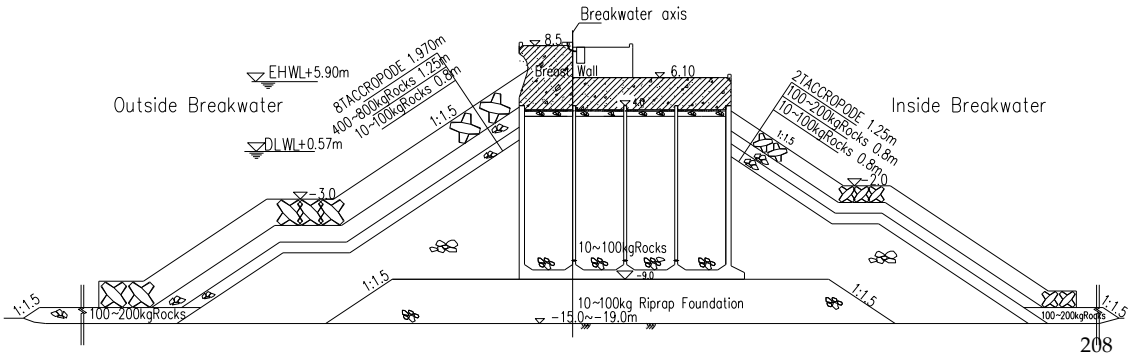


Figure 3. Cross-section of the transition of the different structures.

2.2. Model design

The whole 885.4 m breakwater was simulated, including the vertical caisson structure 300 m at the sea side and the slope-type armor structure 585.4 m near to the shore. According to the relevant provisions of the Technical Code for Simulation Test of Port and Waterway Engineering (JTJ/T231-2021) [38], the normal model was adopted, which was designed according to the Froude number similarity law. The geometric scale of the model was L_r = 1:36; the time scale was $T_r = L_r^{1/2}$; the weight scale was $M_r = L_r^3$; the wave force scale was $F_r = L_r^3$; the pressure scale was $P_r = L_r$; and the wave height scale was $H_r = L_r$.

The test was carried out in a 40 m wide and 50 m long harbor basin equipped with 10 movable irregular wave makers (4 m/set). The wave-making capacity at the maximum wave-making depth was 0.8 m, the wave height was 0~0.3 m, and the period was 0.5~4.0 s. In order to reduce the wave boundary reflection, wave absorbers were set around the harbor basin. For the model making, the terrain within the simulation range was made using the pile point method, with a 1.0 × 1.0 m grid layout. For the local steep terrain, the method of the densities of the pile points was adopted, and the elevation was controlled by a level. All errors met the requirements of the test specification; for the simulation of the vertical caisson, plastic plates were used to make and reinforce the internal structure. The size deviation was controlled to within ±1.0 mm. At the same time, in order to ensure that the center of gravity and mass of the caisson were similar to the original, iron blocks were added as counterweights; the armor blocks and stones were simulated and selected according to the gravity scale, and the quality deviation was controlled to within ±10%. See Figure 4 for the model's layout.



Figure 4. Layout plan of the breakwater transition on the model.

2.3. Test condition design and environmental simulation

1. Water level conditions: In order to reflect the influence of overtopping on stability and wave force, two water levels of+5.90m and+0.57m are selected for the test.
2. Wave conditions: According to the distribution of wave frequency in the open sea and the consideration of the most unfavorable waves, four angles, β=5 °, 15 °, 35 ° and 75 °, are selected between the wave incidence direction and the axis of the breakwater. See Table 1 for wave elements.(Note:the definition method of $\beta$is the same above,see Figure 2 for details). See Table 1 for the test conditions.

Table 1. Test conditions.

Type	Wave direction	*W.L* (m)	$H_{1\%}$ (m)	H_s (m)	T_m (s)
Prototype value	5°, 15°, 35°, 75°	+5.90	6.77	4.88	8.9
		+0.57	5.24	3.83	8.9
Model value	5°, 15°, 35°, 75°	+0.16	0.19	0.14	1.48
		+0.02	0.15	0.11	1.48

NOTE:*W.L* is the water level, and $H_{1\%}$ is wave height with 1% cumulative frequency; H_s is the significant wave height; T_m is the average period;the same below.

Wave simulation: An irregular wave was adopted, and the JONSWAP spectrum was adopted ($\gamma = 3.3$). The simulation of each test condition included no fewer than 1000 waves.

The overtopping volume was measured by the self-developed automatic water collection device. The water was weighed and converted into volume and then converted into the prototype to obtain the average overtopping volume per unit length per unit time.

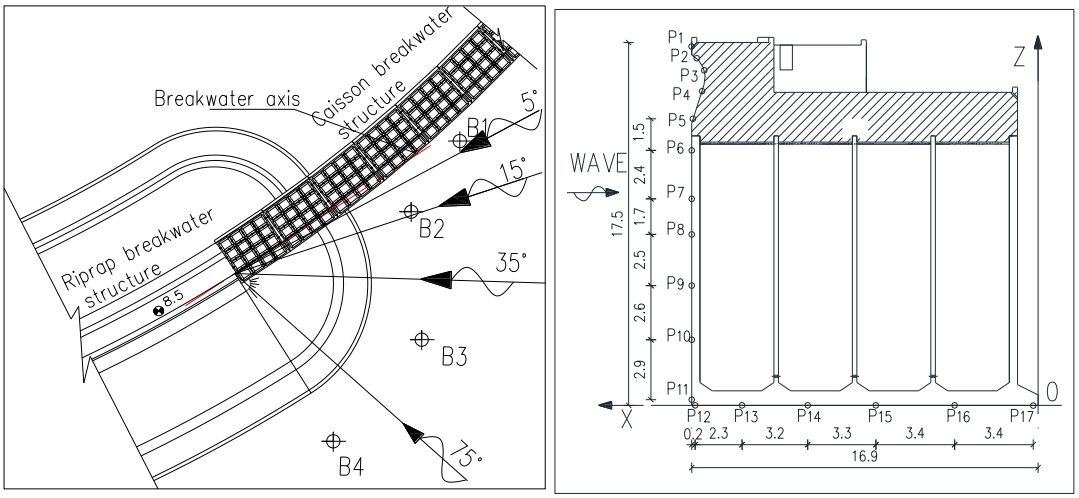
2.4. Layout of measuring points

In order to monitor the wave height change caused in the transition zone of the breakwater by the wave energy concentration and the backwater, four wave height sensors (B1~B4) are arranged, as shown in Figure 5a, and the independently developed TK2008 wave height acquisition system is used for wave surface monitoring and wave height analysis.

For the measurement of the wave force on the caisson at the breakwater transition, the caisson at the exact transition with the sloping embankment was selected, and 17 measuring points (P1~P17) were arranged at the bottom of the caisson and at the side facing the wave. See Figure 5(b) for the layout of the measuring points. The TK2008 dynamic pressure measurement system was used for the collection and analysis. Finally, the horizontal force (*F*x) and buoyancy force (*F*u) on the caisson was obtained by the point pressure integration of Equation (9).The specific method is as follows: during the test, under the condition of still water, zero all measuring points. For measuring points below the still water surface, the hydrostatic pressure at this time is taken as the zero point of the corresponding measuring point, and for measuring points above the still water surface, the atmospheric pressure at this time is taken as the zero point. The pressure value collected in the test is the difference between the actual pressure of the measuring point and the corresponding pressure of the measuring point at the time of zero calibration, that is, the wave hydrodynamic pressure received (the buoyancy result given in the test does not include the hydrostatic buoyancy).

$$F_j(t) = \sum p(t)\, S_j \quad (j = X, Z) \tag{9}$$

where $F_j(t)$ is the wave force in the X and Z directions; $p(t)$ is the pressure of each measuring point; S_j is the projected area of the area occupied by each measuring point in the X and Z directions，See Table 2 for details.



(**a**) (**b**)

Figure 5. Layout of the measuring points and definition of the coordinate system (unit: m): (**a**) arrangement of the wave height measuring points; (**b**) arrangement of the pressure measuring points.

Table 2. Representative area of pressure measuring points

Point	Sj(m²)	Point	Sj(m²)
P1	29.9	P10	97.2
P2	25.2	P11	70.2
P3	33.5	P12	51.8
P4	41.8	P13	103.0
P5	35.3	P14	118.4
P6	86.0	P15	126.4
P7	79.6	P16	132.1
P8	75.2	P17	74.9
P9	83.5	/	/

3. Results

3.1. Analysis of the wave characteristics change law

Based on the special position of the transition of the breakwater, the internal concave angle was formed by two structures. When the waves were incident at different angles, complex hydrodynamic conditions, such as the obvious wave energy concentration, backwater, and overtopping, formed. Especially at a high water level, the backwater will cause the waves to directly cross the top of the dike. Under the wave action of low water level, although there is no overtopping at the top of the embankment, the wave energy superposition is more intense than that of high water level., the energy generated by the concentrated release of wave energy is rotated out of breakwater transition, a huge negative pressure vortex will form on the outer surface of the arc, as shown in Figure 6.

The wave overtopping was collected under the action of 5 °, 15 °, 35 °, and 75 ° waves at the high water level, and compare the calculation results of overtopping volume formula (10) in the Hydrological Code for Ports and Waterways (JTS 145-2015) [41] and the fitting formula (11) proposed by Van der Meer [42], the formula (7) is used to calculate the reduction coefficient of angle influence overtopping, as shown in Table 3. It can be seen from the table that: ① compared with the results of the overtopping at different angles, the 35 ° wave action was the largest; ②The calculation results of Chinese stand-

ards and Van der Meer are smaller than the test results, but there is little difference between the two results.③ It can be concluded that in the special area of the connection section, when the design adopted the formula in the specification, a correction factor of 1.56~1.95 should be multiplied on the basis of the calculated results.



(**a**) (**b**)

Figure 6. Overtopping and vortex phenomenon at the transition under the action of waves: (**a**) overtopping at a high water level; (**b**) diffracted by the sector at a low water level.

$$Q = 0.07^{H_c'/H_s}\exp\left(0.5-\frac{b_1}{2H_s}\right)\sigma K_A\frac{H_s^2}{T_P}\left[\frac{0.3}{\sqrt{m}}+\tanh\left(\frac{d}{H_s}-2.8\right)^2\right]\ln\sqrt{\frac{gT_P^2m}{2\pi H_s}} \quad (10)$$

where Q is the overtopping amount per unit of time and width; H_c' is the height above the static water surface; b_1 is the front shoulder width of the slope; σ is the empirical coefficient, taken as 0.6; K_A is the influence coefficient of the slope structure, taken as 0.45; T_p is the spectral peak period; m is the slope gradient coefficient; and g is the weight acceleration.

$$\frac{Q}{\sqrt{gH_s^3}} = 0.09exp\left[-\left(1.5\frac{H_c'}{H_s r_f r_\beta r_v}\right)^{1.3}\right] \quad (11)$$

Where: r_f is the armor influence coefficient,for Accropode, a value of 0.46[42].r_β is the influence coefficient of wave incidence angle, 1.0 for normal incidence.r_v is the influence coefficient of wave wall.

Table3. Wave overtopping at the transition of the breakwater.

Wave direction	Q(m³·(m·s)⁻¹)			Correction factor	
	Test value	Calculated value			
		Chinese Standards	Van der Meer	Chinese Standards	Van der Meer
5°	0.056	0.031	0.036	1.82	1.56
15°	0.134	0.069	0.082	1.95	1.63
35°	0.345	0.205	0.220	1.68	1.57
75°	0.274	0.156	0.145	1.76	1.89

The impact of the wave energy concentration at the breakwater transition was further analyzed, and the change rules of the wave height and wave crest height in this area under the action of 5 °, 15 °, 35 ° and 75 ° waves were collected, and the results obtained from the wave crest height calculation Equation (12) in the standards [41] were com-

pared, as shown in Table 4. It can be seen from the table that ①Law of wave height variation, it was 1.21~2.05 times higher than the design wave height due to the fact of nonlinear effects, especially 35 ° wave acted, and The composite wave height is 2.05 times of the incident wave height.② Variation law of wave crest elevation, the test value of the wave crest height was 1.29~1.97 times the standard calculation value. It can be concluded that the increase in the wave height was the main reason for the failure of the connection section in the project. Therefore, in the special area of the connection section, when the design adopts the standard formula for calculation, an adjustment coefficient of 1.21~2.05should be multiplied on the basis of the calculation results.

$$\eta_{1\%} = \frac{H_{1\%}}{2} + \frac{\pi H_{1\%}^2}{2L_S} \frac{\left(\cosh\frac{2\pi d}{L_S}\right)\left(\cosh\frac{4\pi d}{L_S}+2\right)}{4\left(\sinh\frac{2\pi d}{L_S}\right)^3} \quad (12)$$

where $\eta_{1\%}$ is the height of the wave crest; L_S is the effective wave length.

Table4. Results of the wave height and wave crest height.

Wave	Point	*W.L* (+0.57m)			*W.L* (+5.90m)		
		Maximum wave crest height			Maximum wave crest height		
		Test value	Calculated value	Correction factor	Test value	Calculated value	Correction factor
5°	B1	5.01	3.74	1.34	4.79	3.66	1.31
	B2	5.60		1.50	5.80		1.58
	B3	5.31		1.42	5.35		1.46
	B4	4.96		1.33	4.71		1.29
15°	B1	5.84	4.21	1.39	5.79	4.05	1.43
	B2	7.08		1.68	6.91		1.71
	B3	6.15		1.46	6.04		1.49
	B4	5.99		1.42	5.79		1.43
35°	B1	7.33	4.77	1.54	7.75	4.86	1.59
	B2	8.90		1.87	9.32		1.59
	B3	7.66		1.61	8.49		1.59
	B4	7.12		1.49	7.63		1.59
75°	B1	9.70	4.93	1.97	8.74	4.73	1.85
	B2	9.17		1.86	8.43		1.78
	B3	8.09		1.64	7.60		1.61
	B4	7.55		1.53	6.58		1.39

3.2. Analysis of the force variation law of the vertical caisson

3.2.1. Variation law of the wave force

According to the test, the caisson was subjected to the wave force, which was mainly composed of the pressure generated by the hydrostatic pressure and the instantaneous wave impact force. The wave force results under the wave actions of 5 °, 15 °, 35 °, and 75 ° angles were collected, and the results of the calculation of Equations (13)~(17) under the conditions of $H/L \geq 1/30$ and d/L = 0.139~0.2 in the specification[41] were compared, and calculation results of the internationally accepted Goda Equation (18)~(27) are used for comparison, Goda Equation[18,19] does not give the calculation formula of wave forces at different angles, so the wave forces at different angles are calculated by using

the calculation results of wave forces under the action of normal waves and combining Equation (15),See Table 5 for comparison results of wave forces.

It can be seen from the table that ① Compared with wave action at different angles, 75° produces the largest wave force and 15° produces the smallest, and the maximum horizontal force and buoyancy were F_{xmax} = 935.6 kN and F_{umax} = 419.1 kN, respectively. ② Compared with the wave action at different water levels, the wave force generated at low water level is greater than that at high water level. The main reason is that when compared with the low water level, the waves at the high water level produce a large number of overtopping waves, which leads to the weakening of wave energy; ③The wave force calculation results of Chinese Standard and Goda Equation are smaller than the test results, but the comparison between the two wave force calculation formulas shows that Chinese Standard is greater than Goda Equation at small angles, and Goda Equation is greater than Chinese Standard when it is close to the normal direction.④ Compared with the standard calculation formula, the test result was 1.08~1.55 times the calculated value. It is analyzed that the reason for the deviation was that the calculation formula considers the reduction coefficient (k_p) of oblique incidence;and coefficient(k_p) was less than 1.0. The product of the two factors ultimately leads to a further smaller calculated value. It can be concluded that for special areas, the wave force on the caisson under oblique wave action is not reduced, but multiplied by an amplification factor, which is 1.13~1.6 according to this test.

$$F_x = 0.5k_p[(H+\eta+d_1)(p_b+\gamma d_1)-\gamma d_1^2] \quad (13)$$

$$F_u = 0.5k_p B p_b \quad (14)$$

$$k_p = 0.5(1+\sin(\beta-22.5°)) \quad (15)$$

$$p_b = p_s - \left(p_s - \frac{\gamma H}{\cosh\frac{2\pi d}{L}}\right)\frac{d_1}{d} \quad (16)$$

$$p_s = \left(\frac{\gamma H}{\cosh\frac{2\pi d}{L}} + \gamma d\right)\frac{H+\eta}{d+H+\eta} \quad (17)$$

where:p_d is the pressure at the toe of the caisson at the sea side; p_s is the static water surface pressure; and d_1 is the water depth on the rubble foundation bed.

$$F_x = 0.5B[(P_s+P_b)d_1+(P_s+P_m)h_c^*] \quad (18)$$

$$F_u = 0.5\alpha_1\alpha_3 B\gamma H \quad (19)$$

$$P_s = (\alpha_1+\alpha_2)\gamma H \quad (20)$$

$$P_d = P_s/\cosh(2\pi d/L) \quad (21)$$

$$P_b = \alpha_3 P_s \quad (22)$$

$$P_m = \begin{cases} P_s(1-h_c/\eta^*), \eta^* > h_c \\ 0, \qquad\qquad \eta^* \le h_c \end{cases} \quad (23)$$

$$\alpha_1 = 0.6+0.5\left[\frac{4\pi d/L}{\sinh(4\pi d/L)}\right]^2 \quad (24)$$

$$\alpha_2 = min\left[\frac{d-d_2}{3d}\left(\frac{H}{d_2}\right)^2, \frac{2d_2}{H}\right] \quad (25)$$

$$\alpha_3 = 1-\frac{d_1}{d}\left[1-\frac{1}{\cosh(2\pi d/L)}\right] \quad (26)$$

$$h_c^* = min(\eta^*, h_c) \quad (27)$$

Where:$\eta^*$is the height between the zero pressure point and the static water surface， When the wave is incident in a normal direction:$\eta^* = 1.5H$;α_1,α_2,$\alpha_3$are correlation coefficients.

Table5. Forces on the caissons calculated by tests and specifications under different conditions.

W.L	Wave direction	F_x/kN					F_u/kN				
		Test value	Calculated value		Correction factor		Test value	Calculated value		Correction factor	
			C-S	G-E	C-S	G-E		C-S	G-E	C-S	G-E
+5.90m	5°	445.5	320.5	313.7	1.39	1.42	228.3	191.8	184.1	1.19	1.24
	15°	654.2	457.5	503.2	1.43	1.30	292.9	242.1	227.1	1.21	1.29
	35°	718.0	448.8	531.9	1.60	1.35	278.0	210.6	237.6	1.32	1.17
	75°	787.1	521.3	558.2	1.51	1.41	337.8	263.9	270.2	1.28	1.25
+0.57m	5°	489.7	371.0	333.1	1.32	1.47	289.9	256.5	239.6	1.13	1.21
	15°	644.3	477.3	473.8	1.35	1.36	349.0	277.0	283.7	1.26	1.23
	35°	835.5	535.6	668.4	1.56	1.25	358.5	261.7	267.5	1.37	1.34
	75°	935.6	588.4	673.1	1.59	1.39	419.1	332.6	358.2	1.26	1.17

Noter:C-S stands for Chinese standards;G-E stands for Gode Equation.

3.2.2. Variation law of the maximum wave pressure

1. Pressure distribution at the ~~moment~~ of the maximum wave force

According to the statistics of the pressure distribution law of each measuring point, there was a phase difference in time when each measuring point was subjected to the maximum pressure during the wave action. At the same time, the pressure generated at each measuring point corresponding to the time when the caisson was subjected to the maximum wave force was not necessarily the maximum pressure. In order to further understand the relationship between the force and pressure, the caisson subjected to the maximum wave force at 75 ° wave condition was selected. The statistical relationship between the two is shown in Figure 7 and Figure 8. It can be seen from the figure ① most of the pressure between the two occurs at different times, and the synchronization rate was less than 5%; ② at the moment of the maximum horizontal force, the pressure at measuring point P4 was the largest, with a P_{xmax} = 57.58 kPa, and the buoyancy force at the bottom of the caisson was the largest,measuring point P12 was the largest, at P_{umax} = 30.22 kPa, and the pressure distribution at the whole bottom was trapezoidal.

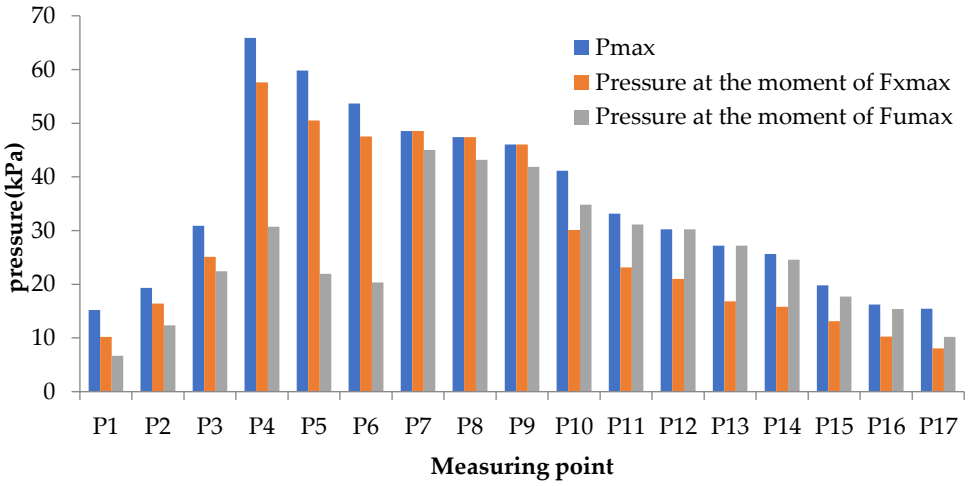
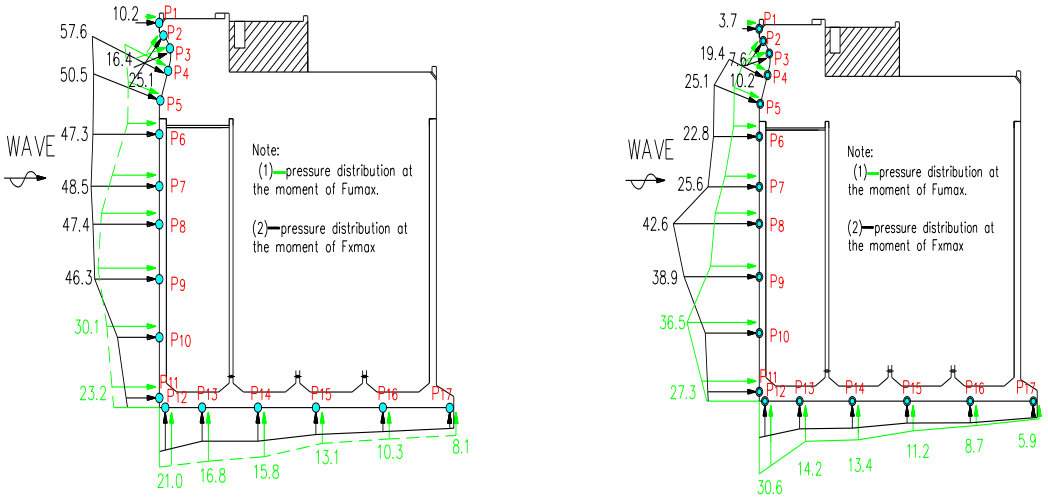


Figure 7. Synchronization rate of P_i and P_{max} at the time of the maximum wave force.



(**a**) (**b**)

Figure 8. Layout of the measuring points and definition of the coordinate system (unit: m): (**a**) arrangement of the wave height measuring points; (**b**) arrangement of the pressure measuring points.

2. Distribution law of the maximum pressure at each measuring point

The maximum pressure results of measuring points P1~P17 were collected, and compared with the calculation results of the pressure Equation (28) in the specification [41]. See Table 6 for the statistics. It can be seen from the results in the table that① The test value is 1.02~1.29 times of the calculated value;② tThe wave impact pressure on the wave side of the caisson is greater than that on the bottom of the caisson. Therefore, in the special area of breakwater, when the designer adopts the standard formula for calculation, It is necessary to multiply the design value by a factor of 1.27~1.42.

Table6. Comparison of the test and calculated maximum pressure results.

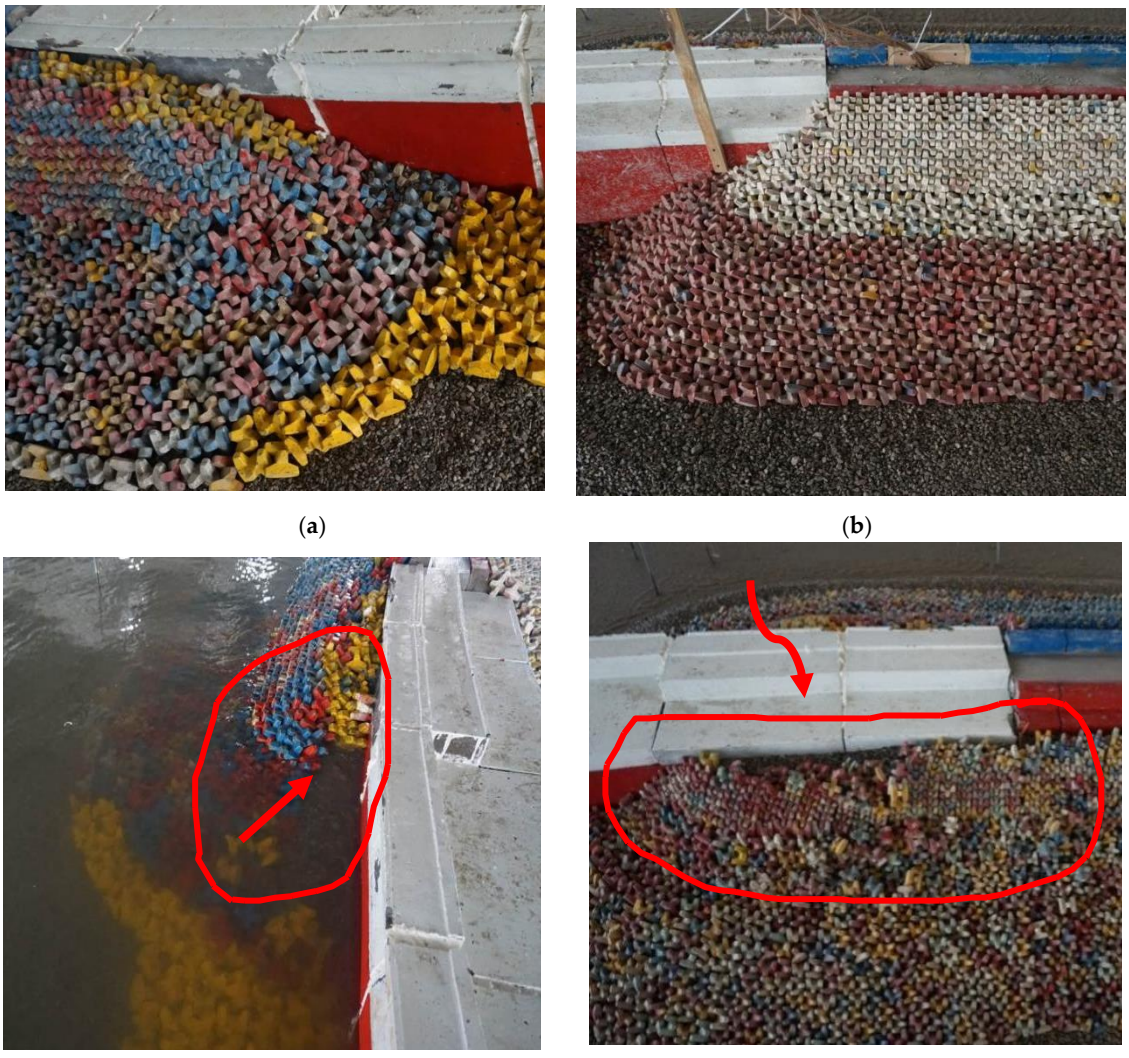
WL	Point	Pressure (kPa)			Point	Pressure (kPa)		
		Test value	Calculated value	Correction factor		Test value	Calculated value	Correction factor
+5.90m	P1	15.2	12.5	1.22	P10	41.1	37.1	1.11
	P2	19.3	16.9	1.14	P11	33.2	31.0	1.07
	P3	30.9	25.8	1.20	P12	30.2	26.8	1.13
	P4	65.9	55.5	1.19	P13	27.2	25.8	1.05
	P5	59.8	50.3	1.19	P14	25.6	22.8	1.13
	P6	53.7	42.9	1.25	P15	19.8	17.1	1.16
	P7	48.5	37.9	1.28	P16	16.2	12.9	1.25
	P8	47.4	38.4	1.23	P17	15.5	12.8	1.22
	P9	46.1	41.0	1.13	/	/	/	/
+0.57m	P1	1.1	1.0	1.13	P10	40.1	33.8	1.19
	P2	9.3	8.5	1.09	P11	38.9	32.3	1.21
	P3	10.7	8.3	1.29	P12	25.7	22.7	1.13
	P4	11.2	9.2	1.22	P13	20.2	19.5	1.04
	P5	15.5	12.8	1.22	P14	15.3	14.4	1.06
	P6	22.5	20.5	1.10	P15	14.4	14.2	1.02
	P7	43.8	38.8	1.13	P16	10.0	9.2	1.09
	P8	46.7	42.2	1.11	P17	3.1	3.0	1.04
	P9	42.1	39.6	1.06	/	/	/	/

$$\frac{p_{1\%}}{\gamma H_{1\%}} = 4.5\left(1-\frac{\Delta h}{\eta_{1\%}}\right)^{0.3} e^{-0.9\left(\frac{\Delta h}{\eta_{1\%}}-0.75\right)^2} \quad (28)$$

Where:$p_{1\%}$is the pressure under the action of 1% wave height with cumulative frequency.Δh is the height from the bottom of the panel to the static water level.$\eta_{1\%}$ is the height of the wave crest corresponding to $H_{1\%}$ wave height above the static water surface.

3.3. Analysis of the stability variation law of the armor block

Through the test, it was found that the instability location of the Accropode at the breakwater transition was mainly in two areas: ①the weak area where the sector arc of the sea side slope engages with the Accorpode at the vertical caisson; ②the overtopping impact area at the corner of the harbor side revetment and the top of the breakwater. See Figure 9 for the instability of the Accropode.



(**a**) (**b**)

(**c**) (**d**)

Figure 9. Instability area of Accropode at the transition. (**a**) ,(c)Comparison of 8T Accropode at sea side before and after ;(**b**),(d) Comparison of 2T Accropode block at port side before and after

Through wave action at different water levels, the stability results of armor are obtained at the breakwater transition, and compared with the calculation results of equations (29) and (30) required in the Code for Design of Breakwater and Revetment (TJS154-2018) [43]. The comparison results are shown in Table 7. It can be seen from the results in the table that: ① Under the action of waves, the 2T accropode designed at the

port side is unstable and optimized to 8T stability; The 8T accropode designed at the sea side is unstable and optimized to be 12T stable.② Compared with the effect of different wave incidence angles on stability, 35° wave action is the most unfavorable for the sea side protection, 75° wave action is the most unfavorable for the harbor basin protection.. ③ The wave force calculation results of Chinese Standard and Rock Manual Equation are smaller than the test results, but the comparison between the two wave force calculation formulas shows that Chinese Standard is greater than Rock Manual Equation at small angles, and Rock Manual Equation is greater than Chinese Standard when it is close to the normal direction.④The test results were compared with the code calculation and design values, and the deviation from the code formula calculation using the reduction coefficient $K_{D.\beta}$ was 1.47~2.50 times, and the deviation from the design value was 1.0~1.5 times. It can be concluded that for special areas, the stable weight of amor block under oblique wave action is not reduced, but multiplied by an amplification factor, which is 1.47~2.50 according to this test.

$$W = 0.1\frac{\gamma_b H^3}{K_D\left(\frac{\gamma_b}{\gamma}-1\right)^3 \cot\alpha} \quad (29)$$

$$K_{D.\beta} = \frac{K_D}{\sin^k(\beta-22.5^\circ)} \quad (30)$$

Where:$K_D$is the stability coefficient, taken as 16(Note:according to Chinese specifications, 15-18 is selected for Accropode , and the middle value is selected for this calculation); k is the test coefficient, taken as 1.50.

Table7. Stability weight of Accropode tested and calculated under different wave angles.

Wave Direction	Test stable weight of Accropode		Calculated stable weight of Accropoder			Design stable weight of Accropode			
	Outside (T)	Inside (T)	$K_{D.\beta}$	All area (T)	Correction factor	Outside (T)	Inside (T)	Correction Factor	
								outside	inside
5°	8.0	6.0	31.6	3.2	2.50	8.0	2.0	1.0	3.0
15°	10.0	6.0	23.7	4.3	2.33	8.0	2.0	1.3	3.0
35°	12.0	6.0	19.4	5.6	2.14	8.0	2.0	1.5	3.0
75°	10.0	8.0	15.2	6.8	1.47	8.0	2.0	1.3	4.0

4. Discussion

Based on the above experimental research results, it is found that the following aspects need to be further improved and supplemented in the follow-up study during the experiment:(1) This study only considers the single dynamic condition of waves, but there is the influence of tidal current under actual natural conditions, and it is easy to form vortex and back-flow at the breakwater transition. The next step is to carry out the research under the wave-current coupling at the transition of the breakwater.(2) For the influence of water level, only high water level and low water level are considered. Due to the difference of water level, different breaking forms and breaking positions of incident waves will be formed. According to the requirements of "Code for Design of Breakwater and Revetment" (JTS154-2018), the weight of armor in the crushing area should be increased by no less than 25%.Therefore, the wave breaking caused by the change of water level will also have an increased impact on the stable weight of the armor block, and it is worth further studying its change law. (3)For the design of the weight of the armor in the special area of the breakwater transition, the amount of overtopping caused by backwater is large, so it is recommended that the same weight of the armor be used as far as possible for the inside and outside of the breakwater; The complex hydrodynamic conditions in these special areas need the attention of designers.(4) At the early stage of breakwater design, the value is calculated by the standard formula, but in order to ensure the structural safety, physical model tests should be carried out as far as possible to check, so as to obtain more reasonable design values.

5. Conclusions

Transition zone with different structural design for breakwater, and the failure accident occurs in the actual project. Based on the few research results on the stability and wave force at the transition zone, and the difficulty in taking design parameters, a physical model test with a scale of 1:36 was carried out. The multi wave action of 5°,15°,35°and 75° is simulated in the test, which reveals the wave characteristics, mechanical properties and failure mechanism of the transition zone:

(1) For the unfavorable hydrodynamic environment characteristics of the breakwater transition, the maximum overtopping volume is 0.345m^3（m·s）$^{-1}$, the maximum specific wave height is 2.05 and other key parameters are obtained. Compared with the calculation results of Chinese standard formula and Van der Meer empirical formula, the maximum overtopping volume and wave crest height are 1.95 and 1.39 times of the latter respectively.

(2)For the wave force on the caisson is directly proportional to the incident wave direction angle and inversely proportional to the water level, that is, the wave action at low water level β=75° is the largest, and the horizontal force and buoyancy force are F_{xmax}=935.6 kN and F_{umax}=419.1 kN respectively; Compared with the calculation results of Chinese code formula and Goda empirical formula, the maximum wave force is 1.60 times of the latter.

(3)For the instability mechanism of the Accropode at the transition of the breakwater, it is mainly caused by the poor connection between the armor block and the caisson, as well as the wave energy concentration and other adverse factors.

(4)For the weight of the Accropode, the designed weighing 2T and 8T is unstable, and it is stable after optimization test to 8T and 12T. Compared with the calculation results of the Chinese code formula, the maximum test result is 2.50 times of the latter; Therefore, for special areas, the stable weight of amor block under oblique wave action is not reduced, but multiplied by an amplification factor, which is 1.47~2.50 according to this test.

The research results solve the practical problems. At the same time, the overtopping volume, wave height and wave force obtained from the test in the special area of the breakwater transition have a large deviation from the design value. Therefore, it is very necessary to carry out physical model tests for major project construction.

Author Contributions: G.S.: data collection, model design and testing, and data analysis; L.Z.: model design and testing, Paper preparation, wave force data processing and analysis; Y.T.: Testing, wave overtopping collection, wave height data processing and analysis; Y.J.: Stability test of armor block, including design scheme and optimization scheme, data processing and analysis; S.G.: series group model testing, test instrument debugging, test terrain processing, and data verification. All authors have read and agreed to the published version of the manuscript.

Funding: Please add: This study was financially supported by the National Natural Science Foundation of China (52101316) special fund for central scientific research institutes (TKS20210110, TKS20220301, and TKS20220110) and Tianjin Science and Technology Foundation (Grant No. 21JCQNJC00480).

Institutional Review Board Statement: Not applicable.

Informed Consent Statement: Not applicable.

Data Availability Statement: Data sharing is applicable to this article, as new data were created or analyzed in this study.

Acknowledgments: This physical model test was conducted in the experimental harbor basin of the Tianjin Research Institute for Water Transport Engineering.

Conflicts of Interest: The authors declare no competing interests. The corresponding author is responsible for submitting a competing interest statement on behalf of all authors of the paper.

References

1. WANG, M.R. Preliminary studies on design method of deep-water breakwater. *Port Engineering Technology*, **2010**, 47 (3): 1-7, 41. DOI: 10.3969/j.issn.1004-9592.2010.03.001.
2. XU, P.L. Discussion on stone dumping and filling construction and quality control of deep-water breakwater. *Building Engineering Technology and Design*, **2020** (17): 2392. DOI: 10.12159/j.issn.2095-6630.2020.17.2324.
3. ZHUO, M.C. Research on construction technology of stone dumping and filling of deep-water breakwater. *Real Estate Guide*, **2014** (14): 400-400. DOI: 10.3969/j.issn.1009-4563.2014.391.
4. QIU, X.B.; QIN J.; CHEN, L.Z. Brief analysis on repair design of typhoon damaged breakwater .*Port Engineering Technology*, **2021**, 58 (6): 15-17. DOI: 10.16403/j.cnki.ggjs20210604.
5. JU, J. Damage and cause analysis of port breakwater. *Urban Architecture*, **2014** (35): 307-307. DOI: 10.3969/j.issn.1673-0232.2014.35.281.
6. GE, L. Z. Research Report on Local Wave Physical Model Test of Breakwater Restoration Project after Typhoon "Shanzhu" in 2018; Tianjin Research Institute for Water Transport Engineering: *Danish Hydraulic Institute:* Tianjin, China, **2019**.
7. ZHANG, H. C.; DONG, S.; et al. Experimental study on the action of oblique irregular waves on the head of sloping breakwater. *Water Transport Engineering*, **2013** (4): 20-24. DOI: 10.3969/j.issn.1002-4972.2013.04.004.
8. CHANG, M.; XIA, Y. Q.; ZHANG, H. C.; et al. Discussion on the stable weight of armor block under the action of oblique waves.*PortEngineeringTechnolog*,**2017**,54(1):40-42,47.DOI: 10.16403/j.cnki.ggjs20170109.
9. JIANG, Y.P.; LIU, C.X.; PENG C. Impact of steep slope and gentle slope topography on revetment works under wave action. *Water Transport Engineering*, 2015 (4): 61-65. DOI: 10.3969/j.issn.1002-4972.2015.04.012.
10. SHEN, M. H.; SI, Y. L. The mechanism of damage caused by resonance on the surface of riprap breakwater. *Journal of Waterway and harbor*, **1984**(4):17-22.
11. WU, S.S.; ZHANG, W.; YUAN, H.P. Study on stability characteristics of concrete interlocking row at different parts of bottom protection. *Water Transport Engineering*, **2008**(11):53-57.DOI: 10.3969/j.issn.1002-4972.2008.11.012.
12. Calheiros-Cabral, T.; Rosa-Santos, P.; Taveira-Pinto, F. Hydraulic and Structural Assessment of a Rubble-Mound Breakwater with a Hybrid Wave Energy Converter. *J.Mar. Sci. Eng*. **2021**, 9, 922. https://doi.org/10.3390/jmse9090922.
13. Vicinanza, D.; Contestabile, P.; ~~Quvang Harck Nørgaard, J.;~~ Lykke Andersen, T. Innovative rubble mound breakwaters for overtopping wave energy conversion. *Coast. Eng.* **2014**, 88, 154–170. https://doi.org/10.1016/j.coastaleng.2014.02.004.
14. Kralli, V.-E.; Theodossiou, N.; Karambas, T. Optimal Design of Overtopping Breakwater for Energy Conversion (OBREC) Systems Using the Harmony Search Algorithm. *Front Energy Res*, **2019**, 7, 11. https://doi.org/10.3389/fenrg.2019.00080.
15. TSANG, S. Y.; LIAW, S. R. A Design Short-Crested Wave Force Model for Vertical Deep-water Breakwaters.//*Coastal engineering ASCE:* Tokyo, Japan, 3March – 6 March **2012**; pp. 563-735.
16. Allsop N W H.; Calabrese M.Impact loadings on vertical walls in directional seas.*Pro. Of 26th ICCE*,**1998**:2056-2068.
17. Battjies J A. Effects of short-crestedness on wave loads on long structures. *Applied Ocean Reserch*,**1982**,4(3):165-172.
18. Goda.Y. *Random seas and design marine structures*. Tokyo: University of Tokyo Press, 1985. 116-119.
19. Goda Y, Tabata T. & Yamamoto S "Technical standards and commentaries for port and harbour facilities in Japan" publn. The Overseas Coastal Area Development Institute of Japan, Tokyo,**2002**.
20. CHENG, Y.Z.; XIAO, D.; LIU B.L.; et al. Experimental study on oblique wave forces on submarine pipelines on sandy seabed. *Ocean Bulletin*, **2018**, 37 (1): 113-120. DOI: 10.11840/j.issn.1001-6392.2018.01.014.
21. CHEN, J.; DUAN, Z.H.; CUI, Y.Q.; et al. Experimental Study on Tsunami Local Scour Law in the Entrance Area of Vertical Breakwater. *Ocean Bulletin*, **2017**, 36 (4): 475-480. DOI: 10.11840/j.issn.1001-6392.2017.04.015.
22. FRANCO, C.; ~~VAN, D.;~~ FRANCO, L. Multidirectional wave loads on vertical breakwaters.// *Coastal Engineering Proceedings 1996*.ASCE, **1996**:2008-2021.
23. HONG, G.G.; WEN, F.; WEI, B.Theoretical Model and Random Simulation for Nonlinear Interaction of Irregular Waves with Vertical Wall. *China Ocean Engineering*, **1993**, (3):263-288.
24. MADRIGAL, B.G. Loads on caisson breakwaters in multidirectional random non-breaking seas. *Proceedings of 5th International Conference on Coastal and Port Engineering in Developing Countries.* Cape Town, South Africa, 29 September -2 October **2019**; pp. 1314-1326.
25. LI, B.X.; YU, Y.X.; ZHANG, N.C. Wave force of multi-directional random wave acting on vertical breakwater. *Journal of Dalian University of Technology*, **2004**, 44 (4): 575-581. DOI: 10.3321/j.issn: 1000-8608.2004.04.025.
26. YU, Y.X.; LI, B.X.; ZHANG, N.C.; et al. Wave load of oblique and multi-directional irregular waves acting on straight wall embankment. *Water Transport Engineering*, **2011** (1): 24-28. DOI: 10.3969/j.issn.1002-4972.2011.01.005.
27. HSU, J. C. Short peak wave. Coastal and marine Engineering Manual. Dalian: *Dalian University of Technology Press*, **1922**:69-129.
28. FENTON, J. D. Wave forces on vertical walls. *Journal of Waterway and Port Coastal and Ocean Engineer*, **1985**, 111(4):693-718.
29. WANG, H.L.; ZHAGN, Y.; ZHAO, J. Wave force analysis on small angle change of wave face of vertical breakwater. *Water Transport Engineering*, **2022** (7): 29-38, 44. DOI: 10.3969/j.issn.1002-4972.2022.07.005.
30. HSU, H.C.; CHEN, Y.Y.; CHEN, Y.R.; Li, M.S. Experimental Study of Forces Influencing Vertical Breakwater under Extreme Waves. *Water* **2022**, 14, 657. https://doi.org/10.3390/w14040657.
31. Cuomo, G.; Allsop, W.; Bruce, T.; Pearson, J. Breaking wave loads at vertical seawalls and breakwaters. *Coast. Eng*. **2010**, 57, 424–439. https://doi.org/10.1016/j.coastaleng.2009.11.005.

32. Alam, M.S.; Winter, A.O.; Galant, G.; Shekhar, K.; Barbosa, A.R.; Motley, M.R.; Eberhard, M.O.; Cox, D.T.; Arduino, P.;Lomonaco, P. Tsunami-Like Wave-Induced Lateral and Uplift Pressures and Forces on an Elevated Coastal Structure. J. Waterw.*Port Coastal Ocean Eng*. **2020**, 146, 04020008. https://doi.org/10.1061/WW.1943-5460.0000562.
33. GE, L.; CHEN, H.; CHEN, S.; LIU, H.Y. Experimental Study on Wave Current Characteristics and Stability of the Junction of Artificial Island and Subsea Tunnel. *J. Mar. Sci. Eng*.**2022**, 10, 1525. https://doi.org/10.3390/jmse10101525.
34. ZHANG, H.C.; DONG, S.; LIU, Y.L.; et al The law of oblique wave propagation along vertical breakwater and its influence on the bank slope breakwater. Proceedings of the 15th China Ocean (Coastal) Engineering Symposium: Qingdao, Shandong Province, **2011**, pp: 727-731.
35. GE, L.Z.; LUAN, Y.N.; CHEN,H.B.; et al. Experimental study on stability of breakwater junction block under oblique wave action and wave force on caisson structure .*Oceanographic Bulletin*, **2021**,40 (1): 113-120. DOI: 10.11840/j.issn.1001-6392.2021.01.013.
36. KUAI, Y.R.; QI, M.L.; LI, J.Z. Wave force analysis of bridge substructure near the coast. *Journal of Zhejiang University (Engineering Edition)*, **2018**, 52 (12): 2356-2364. DOI: 10.3785/j.issn.1008-973X.2018.12.014.
37. SHAO, T.Z.; GUO, F.L. Research on the Layout of Artificial Beach Sand Retaining Dike in Rizhao Port Return to Sea Project. *Waterway port*, **2020**, 41 (2): 157-165. DOI: 10.3969/j.issn.1005-8443.2020. 02.005.
38. Ministry of Transport. *Technical Code for Simulation Test of Water Transportation Engineering*; People's Communications Publishing House Co., Ltd.: Beijing, China, **2021**.
39. Goda Y,Suzuki Y. *Estimation of incident and reflected waves in random wave experiments*.Proceedings of the 15th Conference on Coastal Engineering.ASCE,New York,U.S.A.vol(1),**1976**,pp:828-845.
40. TENG B.;GENG B.L.;LIU S.X.*Determining method for the reflection coefficient and the incident angle of oblique waves*.THE OCEAN ENGINEERING.,2006,24(1):19-26. DOI:10.3969/j.issn.1005-9865.2006.01.004.
41. Ministry of Transport. *Code of Hydrology for Harbor and Waterway*; People's Communications Publishing House Co., Ltd.: Beijing, China, **2015**.
42. Bruce,T.;Van der Meer,J. W.;Franco, L.& Pearson,J.A comparison of overtopping performance of different rubble mound breakwater armour.*Proc.30th Int.Conf. on Coastal Engng*.San Diego,ASCE,**2006**.
43. Ministry of Transport. *Code for Design of Breakwater and Revetment*; People's Communications Publishing House Co., Ltd.: Beijing, China, **2018**.